The favoured cluster structures of model glass formers

Jonathan P. K. Doye* and David J. Wales
University Chemical Laboratory, Lensfield Road, Cambridge CB2 1EW, United Kingdom

Fredrik H. M. Zetterling and Mikhail Dzugutov
Department of Numerical Analysis, Royal Institute of Technology, SE-100 44 Stockholm, Sweden
(Dated: February 1, 2008)

We examine the favoured cluster structures for two new interatomic potentials, which both behave as monatomic model glass-formers in bulk. We find that the oscillations in the potential lead to global minima that are non-compact arrangements of linked 13-atom icosahedra. We find that the structural properties of the clusters correlate with the glass-forming propensities of the potentials, and with the fragilities of the corresponding supercooled liquids.

I. INTRODUCTION

There is still much to learn about the nature of the glass transition,[1] and so it is an area of intense current interest. One of the increasingly prominent avenues of research in this field is the computational study of model supercooled liquids and glasses,[2] driven by the increase in computational power that has allowed larger systems to be studied over longer time scales. The advantage of the computational approach is that the configuration of the liquid or glass is directly available, potentially making it possible to understand the basis of the changes that occur as the glass transition is approached in terms of the structure and energy landscape. Indeed, this mode of research has led to an increasing number of new insights, for example, into the relationship between the energy landscape and the properties of supercooled liquids[3,4] (in particular the fragility[5]), the mechanisms of cooperative motion,[6] the growing length scale of correlated motion as the temperature is decreased[7] and whether a thermodynamic transition underlies the glass transition.[8]

One of the basic requirements of a model system to study supercooled liquids and glasses is that it will not crystallize on the relevant time scales. This constraint precludes the use of a monatomic system interacting with simple pair potentials, such as the Lennard-Jones potential, because crystallization can occur relatively easily. Instead, the most commonly used model glass former is a binary Lennard-Jones system developed by Kob and Andersen,[9] However, one drawback of using a binary system is that it is much harder to identify the structural changes that occur on approaching the glass transition. Indeed the nature of the preferred local order in this system has not been systematically studied. Furthermore, a crystalline ground state has recently been discovered for this system.[10] In monatomic Lennard-Jones systems it is relatively easy to detect the presence of any close-packed crystallinity in a sample, but incipient crystallization is much less obvious in a binary system with a complex crystal structure, where the growth rate of any crystalline nuclei is expected to be slow. It is therefore unclear whether incipient crystallization could have contaminated any of the previous studies of the supercooled liquid of the binary Lennard-Jones system. In one case, at least, a low-energy configuration has been generated that shows signs of demixing and crystalline layering.[11]

An alternative approach is to use a monatomic system, but one that has been tailored to prevent crystallization. There have been two notable ways in which this goal has been achieved. In the first, a small term is added to the potential (in this case a Lennard-Jones potential) that is a function of the static structure factor and inhibits ordering.[12] However, under some conditions this method is not completely effective at preventing crystallization.[13] The second approach involves designing a potential that disfavours the close-packed order that is usually favoured by monatomic systems with isotropic pair potentials. Dzugutov achieved this by introducing a maximum in the potential at approximately $\sqrt{2}$ times the equilibrium pair distance (see Figure 1),[14,15] which is the distance between opposite vertices of the octahedra that are intrinsic to close-packing. This maximum causes the preferred local order in the system to be polytetrahedral and icosahedral. Thus, systems bound by this Dzugutov potential are good glass-formers, and exhibit a first sharp diffraction peak and a split second peak in the structure factor,[16] which are common features of metallic glasses. One other interesting feature of this potential is that under certain conditions it can produce a dodecagonal quasicrystal.[17]

It is well known that there is an increasing tendency for local polytetrahedral and icosahedral order in simple liquids as the temperature is decreased.[18–20] Recent results for Dzugutov liquids have shown how this change in local order affects the overall structure of the liquid, and is responsible for the changes in properties as the glass transition is approached. There is low-dimensional growth of icosahedral clusters, which eventually percolate through the system leading to a dramatic increase in the structural relaxation time.[21,22] The described cluster growth leads to two interesting dynamical effects: a pronounced spatial variation of atomic mobility and a breakdown of the Stokes-Einstein relation.

An understanding of this intriguing behaviour can be obtained by examining the structures of isolated clusters.[23] The lowest-energy structures of the clusters

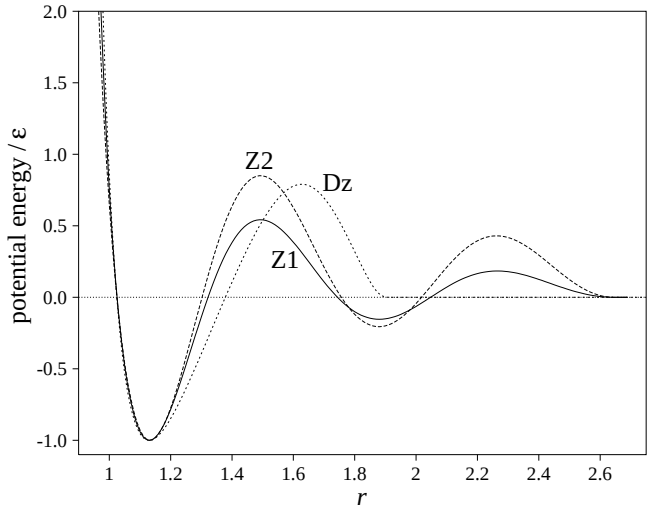

FIG. 1: The potential energy curves of the two new potentials (Z1 and Z2) compared to the original Dzugutov (Dz) potential. To aid comparison of the potentials, the energy is in units of ϵ, the pair well depth for the appropriate potential.

can all be considered as aggregates of linked 13-atom icosahedra. However, these aggregates are not compact and as the size increases they change from chains to rings to porous three-dimensional network structures. Therefore, the clusters show the same tendency for low-dimensional aggregation of icosahedra.

One additional advantage of using a monatomic system to study supercooled liquids is that it is much easier to understand the effect of changing the form of the potential. We can therefore systematically study how properties, such as the glass-forming ability and fragility, depend on the potential. This is the approach we use here.

One justification for the form of the Dzugutov potential is that the maximum resembles the first of the Friedel oscillations that occur for metal potentials. However, further maxima occur in the latter case. Here we investigate two potentials that have two maxima. The crystallization behaviour of one of these potentials (Z1) has already been studied by molecular dynamics simulations[24]—the γ-brass[25] structure resulted—and crystallization patterns of the other pair potential (Z2) will be explored elsewhere.[26] In this paper, we focus on the lowest-energy structures exhibited by clusters bound by these potentials, paying particular attention to the relationship between the observed structures and the form of the potential.

Complementary to these studies of isolated clusters, we also explore the bulk liquids for the two potentials with molecular dynamics. One particular purpose of these simulations is to investigate the liquids' behaviour upon supercooling and their glass-forming abilities. We also compare the lowest-energy structures for the isolated clusters with the coherently structured domains with predominantly icosahedral local order that develop upon supercooling of the bulk liquids. The results we present here will be particularly helpful in rationalizing the role of the pair potential and the related local order in the development of extended transient structures in the supercooled liquids as the glass transition is approached.

TABLE I: Values of the parameters for the Z1 and Z2 potentials. The values of r_c and V_0 are defined by the relations in the text, and only truncated values are reproduced here.

	a	α	k_F	b	σ	n	r_c	V_0
Z1	1.58	-0.22	4.120	4.2×10^8	0.331	18.0	2.64909	0.04682632
Z2	1.04	0.33	4.139	4.2×10^7	0.348	14.5	2.64488	0.13391543

II. METHODS

The two potentials both have the form

$$V(r) = a\frac{e^{\alpha r}}{r^3}\cos(2k_F r) + b\left(\frac{\sigma}{r}\right)^n + V_0 \qquad (1)$$

for $r < r_c$ and 0 otherwise. We use the position of the third minimum in the function as our cutoff distance, r_c, and V_0 is defined through the equation $V(r_c) = 0$, i.e. V_0 acts to shift the potential so that it vanishes at the third minimum, thus making the function and its first derivative continuous at the cutoff. The values of the parameters for the two potentials are given in Table I, and they are plotted in Fig. 1 together with the Dzugutov potential. We denote the two potentials as Z1 and Z2.

The form of the new potentials has a more physical basis than the original Dzugutov potential. The first term has a form similar to that expected for the effective interaction between metal ions when screened by electrons. Friedel oscillations are present with wave-vector, $2k_F$, where k_F corresponds to the wave-vector at the Fermi level. The second term adds a repulsive interaction that suppresses the oscillations at small r. The potentials look similar to the effective pair potentials often derived for metallic systems,[27,28] however in the latter case the potentials are density dependent.

The total potential energy of a cluster interacting with this potential is simply $E = \sum_{i<j} V(r_{ij})$. A cluster structure that has a low energy must have pair distances that lie close to the minima in the potential and that avoid the maxima. The first maximum occurs at $r = 1.320\,r_{\rm eq}$ and $1.318\,r_{\rm eq}$ for Z1 and Z2 respectively, where $r_{\rm eq}$ is the appropriate equilibrium pair separation. The potential still has a large positive value at $\sqrt{2}\,r_{\rm eq}$, thus the possibility of close-packed structures is ruled out, as for the Dzugutov potential. Instead the potential favours polytetrahedral structures that can avoid this maximum; if the tetrahedra are regular, the first next-nearest neighbour distances occur at $r = \sqrt{2/3}\,r_{\rm eq} = 1.633\,r_{\rm eq}$, close to the second minimum at $r = 1.663\,r_{\rm eq}$ (Z1) or $1.659\,r_{\rm eq}$

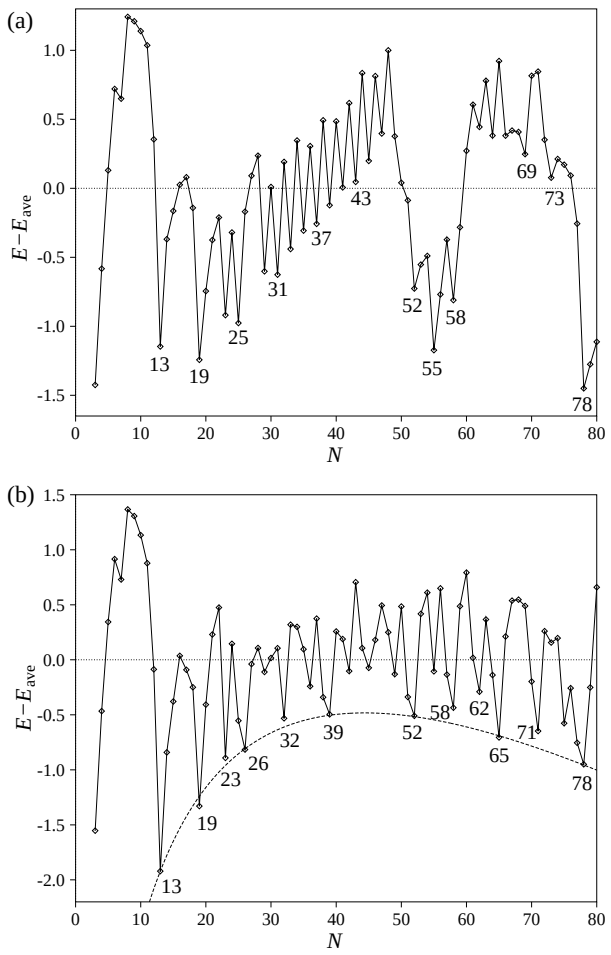

FIG. 2: Energies of clusters interacting with the two potentials. In (a) the energy zero is $E_{\rm ave}^{\rm Z1} = -2.9445\,N + 0.9278\,N^{2/3} - 2.7108\,N^{1/3} + 10.1508$ and in (b) is $E_{\rm ave}^{\rm Z2} = -2.7311\,N + 1.0818\,N^{2/3} - 7.4369\,N^{1/3} + 15.9735$. In (b) the dashed line represents the fit to the energies of the chains of icosahedra occurring at $N = 13n$, $E_{\rm n-icos} = -2.6613\,N - 0.5940\,N^{2/3} + 1.8063\,N^{1/3} + 0.6760$.

(Z2).

As a packing of regular tetrahedra is not achievable in Euclidean space, polytetrahedral structures inevitably involve nearest-neighbour distances that deviate from the ideal value. The energetic penalty for this strain depends sensitively on the width of the potential well. As the first minima of the Z1 and Z2 potentials are somewhat narrower than the Dzugutov potential well (Figure 1), one expects the lowest-energy structures to be non-compact, as for the Dzugutov clusters.[23] This allows the strain energy inherent to compact polytetrahedral forms to be avoided, whilst maintaining polytetrahedral order. This effect can be quantified by matching the curvatures of the potential at $r = r_{\rm eq}$ to that for the Morse potential, which has a single parameter ρ that determines the width of the potential well. $\rho_{\rm eff}^{Z1} = 8.63$ and $\rho_{\rm eff}^{Z2} = 8.89$, which are somewhat larger than the value for the Dzugutov potential ($\rho_{\rm eff}^{Dz} = 7.52$)[23] and much larger than the values of ρ for which the Morse potential has compact polytetrahedral global minima.[29]

We attempted to locate the cluster global minima using the basin-hopping global optimization algorithm.[30,31] Since the Z1 and Z2 potentials vanish beyond a distance r_c, precautions were needed to maintain efficiency. The cluster is placed in a spherical container to prevent atoms evaporating. However, for the structures considered in the present work there can still be a significant amount of empty space in the container. We therefore checked periodically whether the pair energy of any atoms was identically zero. Such atoms were reconnected with the cluster by moving them within the attractive range of their nearest neighbour.

The global minima of these clusters are particularly hard to locate because the oscillations in the potential lead to a rough energy landscape with huge numbers of minima and large energy barriers between different structural forms.[23] Furthermore, the non-compact nature of the global minima means that the volume of configuration space that needs to be searched is much larger than for compact clusters. Due to these difficulties, it would be no surprise if some of the lowest-energy minima that we found at larger sizes are not the true global minima. Indeed, for some sizes we were able to construct lower-energy structures using the physical principles deduced from the structures that we were able to find. However, as we are more interested in the general structural evolution of the global minima with size, rather than the specifics of individual cluster sizes, this is not a serious problem.

III. RESULTS

A. Isolated Clusters

The energies and point groups of the putative global minima for all clusters up to $N = 80$ that we have located for the two potentials are given in Table II. The points files will also be made available online at the Cambridge Cluster Database.[32] In Figure 2 we plot the energies of the global minima in a way that causes particularly stable sizes to stand out. The structures of a selection of these "magic" sizes, and other sizes where interesting high symmetry structures were observed, are depicted in Figures 3 and 4.

As expected, for both potentials the structures exhibited are non-compact arrangements of connected 13-atom icosahedra. For all the particularly stable sizes evident in Figure 2 these icosahedra are complete.

There are three ways in which the icosahedra are linked: (i) two icosahedra can interpenetrate sharing a common fivefold axis, as in the 19-atom double icosahedron; (ii) two icosahedra can share a face as in the 23-atom structure that is the global minimum for both potentials; (iii) two separated icosahedra can be joined by a tetrahedron whose opposite edges are shared with the

TABLE II: Energies and point groups (PG) of the lowest-energy minima located for clusters interacting with the Z1 and Z2 potentials.

	Z1		Z2			Z1		Z2	
N	PG	Energy	PG	Energy	N	PG	Energy	PG	Energy
3	D_{3h}	-2.087454	D_{3h}	-2.248317	42	C_s	-111.113917	C_s	-111.615125
4	T_d	-4.174907	T_d	-4.496633	43	D_{3h}	-114.526364	C_s	-113.534760
5	D_{3h}	-6.363630	D_{3h}	-6.891923	44	C_{3v}	-116.579062	C_1	-116.860294
6	C_{2v}	-8.658495	C_{2v}	-9.439398	45	C_s	-120.057909	C_s	-119.765131
7	D_{5h}	-11.602168	D_{5h}	-12.682192	46	C_s	-122.284996	C_2	-122.234952
8	C_s	-13.873626	C_s	-15.054741	47	C_1	-125.544082	C_1	-124.643068
9	C_{2v}	-16.763730	C_{2v}	-18.089069	48	C_1	-127.783337	C_1	-127.608371
10	C_{3v}	-19.689189	C_{3v}	-21.205084	49	C_s	-131.249095	C_1	-130.709014
11	C_{2v}	-22.642702	C_{2v}	-24.379370	50	D_{2h}	-134.429471	C_1	-132.812275
12	C_{5v}	-26.171418	C_{5v}	-28.242064	51	C_{2v}	-137.399683	C_1	-136.352523
13	I_h	-30.518777	I_h	-32.957039	52	C_{4h}	-140.882324	C_1	-139.240474
14	C_{3v}	-32.585210	C_{3v}	-34.743529	53	C_1	-143.552544	C_1	-141.027989
15	C_{2v}	-35.223551	C_{2v}	-37.132647	54	C_s	-146.333923	C_1	-143.549558
16	C_s	-37.875551	C_s	-39.558764	55	C_s	-149.860950	C_1	-146.978638
17	C_s	-40.662152	C_s	-42.515739	56	C_1	-152.301798	C_1	-148.936593
18	C_s	-43.724272	C_s	-45.495502	57	C_s	-154.749296	C_2	-152.431591
19	D_{5h}	-47.665071	D_{5h}	-49.388337	58	C_{2h}	-158.032574	C_1	-155.443175
20	C_{2v}	-50.006755	C_{2v}	-51.271893	59	C_s	-160.349915	C_1	-157.230650
21	C_1	-52.475722	C_s	-53.433094	60	C_1	-162.641511	C_1	-159.634564
22	C_s	-55.150884	C_s	-55.980724	61	C_1	-165.152433	C_1	-163.117336
23	D_{3h}	-58.697886	D_{3h}	-60.133544	62	C_1	-168.159905	C_1	-166.132881
24	C_s	-60.937135	C_{3v}	-61.878219	63	C_1	-170.671345	C_1	-168.183340
25	D_{5d}	-64.432022	D_{5d}	-65.353500	64	C_2	-173.914159	C_1	-171.393944
26	C_s	-66.463833	D_{2d}	-68.387900	65	C_1	-176.220446	C_1	-174.666612
27	C_s	-69.042269	C_2	-70.379358	66	C_2	-179.608322	C_1	-176.454127
28	C_s	-71.735736	C_{2v}	-72.997963	67	C_1	-182.418355	C_1	-178.831638
29	C_s	-75.412716	C_{2v}	-75.975750	68	C_1	-185.275450	C_1	-181.526788
30	C_s	-77.640330	C_1	-78.606894	69	C_s	-188.283757	C_1	-184.286813
31	D_{5h}	-81.114676	D_{5h}	-81.271817	70	C_1	-190.562830	C_1	-187.676283
32	C_s	-83.136786	C_s	-84.659842	71	C_1	-193.380298	C_1	-190.827932
33	D_{3d}	-86.608012	C_1	-86.557138	72	C_s	-196.722616	C_1	-192.621016
34	C_{3v}	-88.660767	C_s	-89.323678	73	C_s	-199.845668	C_1	-195.425747
35	C_{2v}	-92.153818	C_s	-92.270480	74	C_1	-202.558045	C_1	-198.085004
36	C_s	-94.381048	C_s	-95.348047	75	C_1	-205.448065	C_1	-201.559019
37	D_{5d}	-97.784539	C_s	-97.471834	76	C_i	-208.375341	C_1	-203.939219
38	D_{6h}	-99.874893	C_2	-100.923541	77	C_s	-211.573361	C_1	-207.134890
39	C_s	-103.330875	C_2	-103.814208	78	C_{2v}	-215.615804	C_1	-210.028014
40	C_s	-105.563799	C_1	-105.793804	79	C_1	-218.290788	C_1	-212.027576
41	C_s	-108.883830	C_{2v}	-108.594370	80	C_2	-220.977578	C_1	-213.815040

two icosahedra, as in the 26-atom structure that is the Z2 global minimum. All these ways of linking icosahedra are common in metallic alloys.[33]

These three different modes of linkage leads to a large number of possible icosahedral aggregates, especially at larger sizes. For example, the 55-atom Z1 global minimum involves all three possibilities: there is one pair of interpenetrating icosahedra, one pair of face-sharing icosahedra and three pairs of icosahedra that are bridged by tetrahedra.

For both potentials, beyond $N = 13$ the global minima initially develop into chains of linked icosahedra. For the Z1 potential these chains involve a mixture of both interpenetrating and face-sharing icosahedra, but no icosahe-

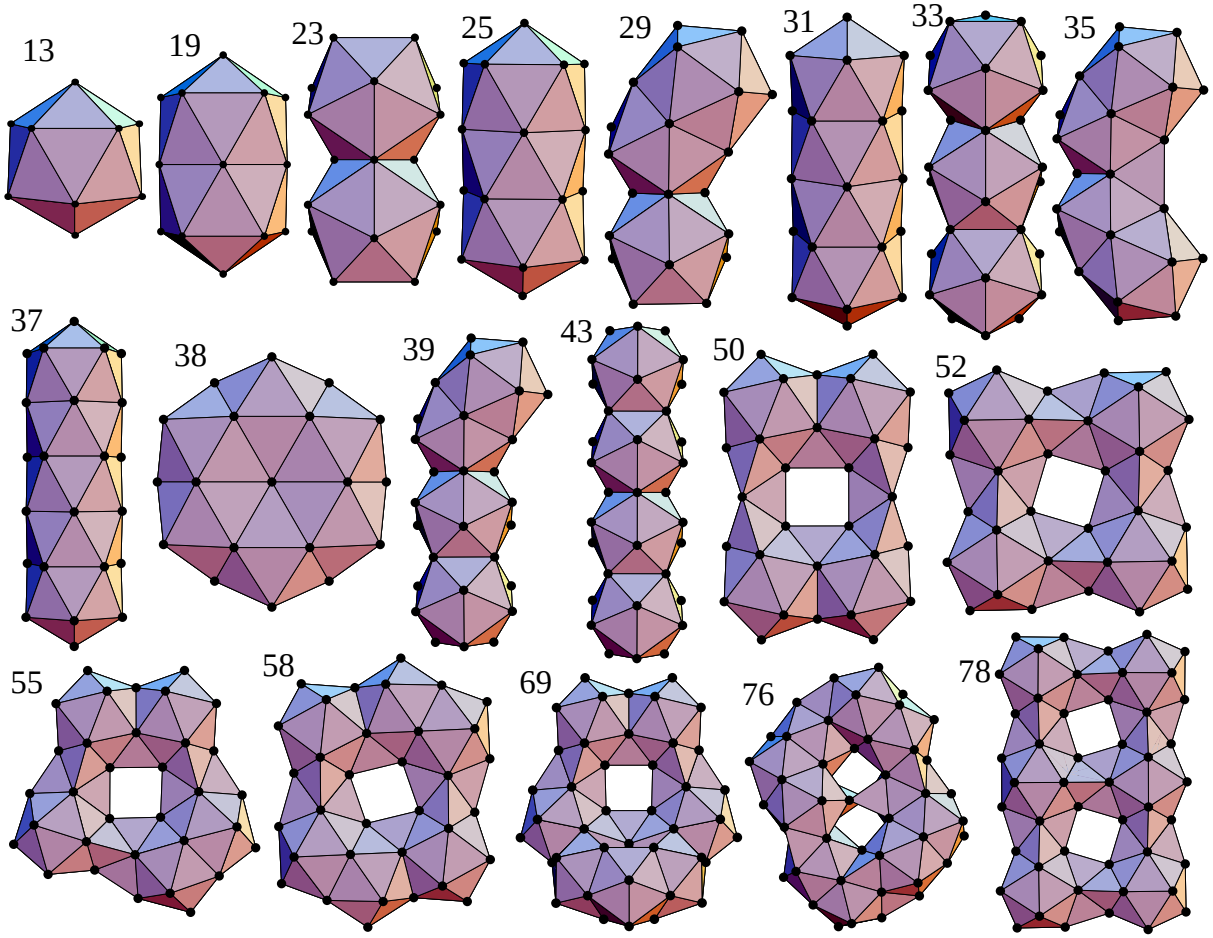

FIG. 3: A selection of Z1 global minima. Each is labelled with the value of N.

dra linked by tetrahedra. Such structures with complete icosahedra are only possible at odd sizes, leading to the odd-even oscillations seen in Figure 2(a) for $N = 29-49$. The only global minimum in this size range that is not chain-like occurs at $N = 38$. It is a disk-like fragment of the Z-phase (one of the Frank-Kasper phases[34,35]), which was particularly stable for the Dzugutov potential.[23] Beyond $N = 50$ the Z1 global minima start to exhibit ring-like structures, and at the largest sizes that we consider they become double rings.

The 52-atom Z1 global minimum is particularly interesting. It is a square array of icosahedra linked through tetrahedra, and it is easy to see how this motif can be repeated to form extended two- and three-dimensional networks of icosahedra. For example, the 78-atom double ring structure is simply formed by the addition of two further icosahedra. Furthermore, two of the 52-atom structures can be placed on top of each other to produce a cubic array of icosahedra at $N = 104$. Although we have not attempted any global optimization at this size, a comparison of the energy of this cluster (-296.947505) with an extrapolation of $E_{\rm ave}$ (a fit to the energies of the putative global minima) suggests that it is extremely stable. This result has two implications. Firstly, the transition to three-dimensional structures is likely to occur for the Z1 potential just beyond the size range we consider. Indeed, the 91-atom structure formed by removal of an icosahedron at one corner of the cube also appears to be particularly stable ($E = -253.432268$). Secondly, it seems plausible that at zero pressure the crystal structure formed by repeating this cubic unit could also be most stable. This crystal would be the same as the $NaZn_{13}$ crystal[33] but with vacancies at the Na sites. This possibility contrasts somewhat with the results of constant volume simulations (corresponding to higher densities) where crystallization to a γ-brass structure[25] was observed.[24]

For the Z2 potential, by contrast, there is a definite preference for icosahedra linked by tetrahedra. Hence, there is a series of stable chain structures that occur at $N = 13n$ (Fig. 2). Furthermore, these are the most stable structures over the whole size range that we study. There is no crossover to two- or three-dimensional networks of icosahedra. When we add a third icosahedron to the 26-atom global minimum, there are five possible positions for it. In fact neither the linear nor the L-shaped

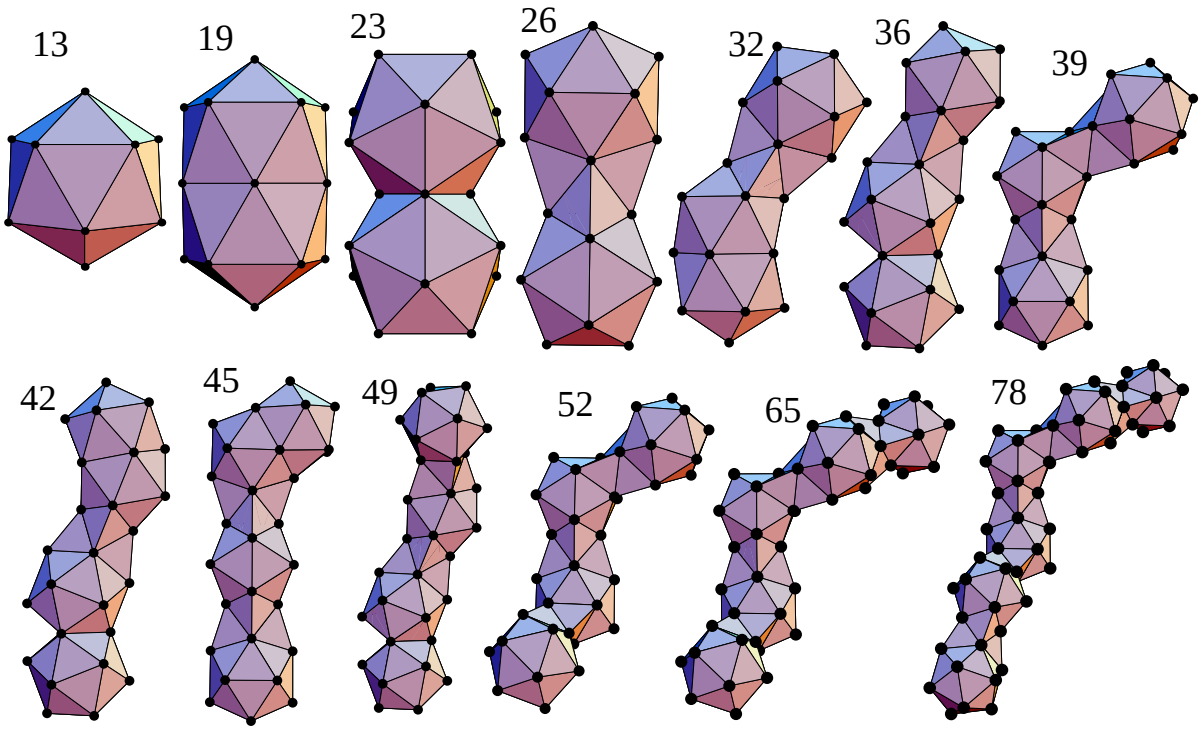

FIG. 4: A selection of Z2 global minima. Each is labelled with the value of N.

configurations are lowest in energy. Instead, the angle between the central atoms of the three icosahedra in the 39-atom global minimum is approximately 120°. This angle might lead one to think that a hexagonal ring could be formed from six icosahedra, but because the linked icosahedra are in different orientations, a flat configuration with four icosahedra is not possible. Instead, the 52-atom global minimum is a bent chain with two 120° angles between the centres, and a 90° torsion angle. It is also noteworthy that the extra linkage between icosahedra in the ring of the Z1 52-atom global minimum is not enough to stabilize this structure, because the Z2 potential so disfavours 90° angles between the icosahedral centres. However, in constant volume bulk simulations for the Z2 potential, the system has been observed to crystallize into a $NaZn_{13}$-like structure with most of the Na sites vacant.[26]

When comparing the behaviour of the structures for the Z1 and Z2 potentials with the Dzugutov clusters, it is clear that the Z1 clusters are the most similar to the Dzugutov clusters. However, the crossovers to two- and to three-dimensional icosahedral aggregates occur at larger sizes for the Z1 potential, and the Dzugutov potential has a greater preference for face-sharing linkages.[23] Therefore, there is an increasing tendency for the clusters to exhibit non-compact, low-dimensional icosahedral aggregates on going from the Dzugutov, to the Z1 and then to the Z2 potential. One can say that these systems become more frustrated,[36] i.e. it becomes increasingly hard to propagate the locally preferred polytetrahedral order freely through space. There is also a modified version of the Dzugutov potential that has been designed to exhibit compact polytetrahedral clusters by giving the potential a wider well that can sustain the inherent strain in these clusters.[37] The effective range parameter for this potential, $\rho_{\rm eff}^{\rm m-Dz}$, is 5.16.

The above series of four potentials therefore provides an ideal opportunity to correlate the properties of the supercooled liquid with the local structure seen in the clusters and the form of the potential. As the potential becomes more frustrated, one would expect a percolating network of icosahedral clusters to develop more rapidly as the temperature is decreased, thus leading to more fragile behaviour,[38] i.e. the structural relaxation time has a super-Arrhenius temperature dependence. Similarly, rearrangements of these icosahedral aggregates are also likely to be especially slow, and thus they inhibit crystallization. So one also expects the more frustrated potentials to be better glass-formers.

It is relatively easy to relate the differences between the structures observed for the different types of cluster back to the form of the potential. First, we shall examine the variations in the tendency to form low-dimensional aggregates. The second maximum in the Z1 and Z2 potentials places an additional constraint on the system, as it is harder to avoid than the first maximum. Distances at roughly $2r_{\rm eq}$ in polytetrahedral clusters (e.g. opposite vertices of an icosahedron) occur near the centre of this maximum (Fig. 5) and so are significantly penalized. The number of such distances is of course larger for a compact

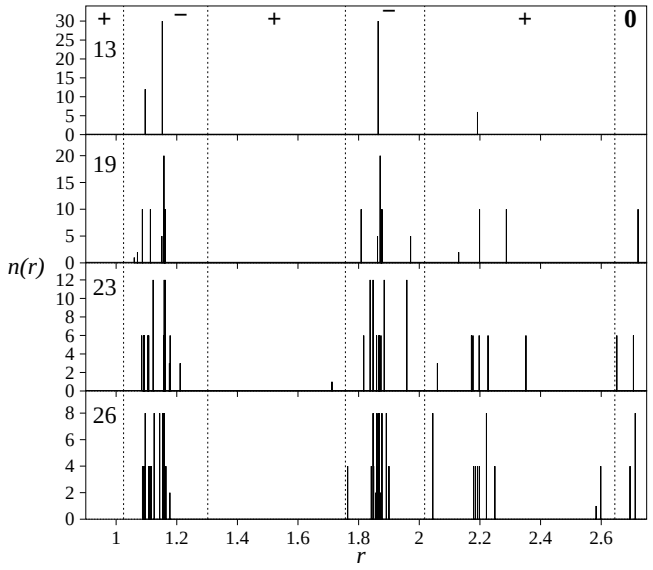

FIG. 5: The number of pairs separated by a distance r, $n(r)$, for the Z2 global minima at N=13, 19, 23 and 26, as labelled. The dotted lines correspond to the distances at which the Z2 potentials changes sign or goes to zero at the cutoff distance.

compact cluster, so the Z1 and Z2 potentials have an extra force driving them towards non-compact geometries over and above that for the Dzugutov potential. This effect is more pronounced for the Z2 clusters, simply because of the larger size of the maximum (Figure 1).

It is also possible to rationalize the preferred types of linkage between the icosahedra. To aid this analysis we have decomposed the potential into five terms

$$E = -n_{\rm nn}\epsilon + E_{\rm strain} + E_{\rm max1} + E_{\rm min2} + E_{\rm max2}, \quad (2)$$

where $n_{\rm nn}$ is the number of nearest neighbours, $E_{\rm strain}$ is the energetic penalty for nearest-neighbour distances that deviate from the equilibrium pair separation,[29] and $E_{\rm max1}$, $E_{\rm min2}$ and $E_{\rm max2}$ are the energies associated with pair distances near to the first maximum, second minimum and second maximum, respectively. The distance criteria used to separate these different contributions are simply the distances for which $V(r) = 0$.

We report the above contributions to the energy for the icosahedron and the three ways of linking two icosahedra in Table III. We also show the pair distribution functions for these structures in Fig. 5. For a given size, the number of nearest neighbours is largest for the interpenetrating icosahedra and smallest for the icosahedra linked by tetrahedra, as would be expected from the relative compactness of the resulting structures.[39] However, to compensate for this effect the interpenetrating icosahedra have the largest strain energy and $E_{\rm max2}$ for a given size and the tetrahedra-bridged icosahedra the smallest.

When comparing the contributions to the energy for the same structure, but for the two potentials, it is clear from Table III that the major changes are in $E_{\rm min2}$ and

TABLE III: The contributions to the energy defined by Equation (2) for the 13-atom icosahedron and the three ways of linking them. All the energies are measured in units of ϵ, the pair well depth for the appropriate potential.

	N	Energy	$n_{\rm nn}$	$E_{\rm strain}$	$E_{\rm max1}$	$E_{\rm min2}$	$E_{\rm max2}$
Z1	13	-43.860	42	1.711	0.000	-4.531	0.959
	19	-68.502	68	4.258	0.000	-8.442	3.682
	23	-84.358	84	5.429	0.088	-10.841	4.965
	26	-94.894	92	3.779	0.000	-11.586	4.913
Z2	13	-43.976	42	1.787	0.000	-6.075	2.312
	19	-65.900	68	4.454	0.000	-11.096	8.742
	23	-80.238	84	6.151	0.162	-14.282	11.730
	26	-91.252	92	4.315	0.000	-15.322	11.755

$E_{\rm max2}$, due to the greater magnitude of the second maximum and minimum for the Z2 potential. Indeed, there is a greater driving force for minimizing $E_{\rm max2}$ for the Z2 potential, and it is this factor that leads to the icosahedra linked by an intervening tetrahedron to be dominant.

Similarly, when linking more than two icosahedra through intervening tetrahedra, 90° angles between the icosahedral centres are disfavoured for the Z2 potential because this introduces some distances between the atoms in the non-adjacent icosahedra that are near to the second maximum.

B. Bulk liquids

The properties of the bulk liquids for the Z1 and Z2 potentials were explored by molecular dynamics simulations of a system of 16 000 particles at a number density ρ=0.84. The simulations focused on the behaviour of these liquids in the supercooled domain. We take as the upper bound of this domain, not the limit of thermodynamic stability (the melting temperature T_m), but the temperature (T_A) below which the liquid begins to demonstrate a set of characteristic dynamical anomalies that are routinely associated with the notion of supercooled liquid dynamics. The most celebrated of these anomalies is the super-Arrhenius slowing down, which is commonly regarded as a defining property of the supercooled liquid state. One purpose of the present molecular dynamics simulations was to explore the glass-forming abilities of the two systems (the notion of the glass-forming ability of a liquid refers to its ability to remain in a state of metastable equilibrium within a temperature domain where it exhibits the super-Arrhenius behaviour and other characteristic features of supercooled liquids). To this end, we subjected each of the two liquids to a step-wise cooling whereby at each temperature step the system was relaxed to the state of apparent equilibrium.

The temperature variation of the diffusion coefficient for both potentials is shown in Fig.6. In both cases, $D(T)$ exhibits a pattern characteristic of fragile glass-formers:

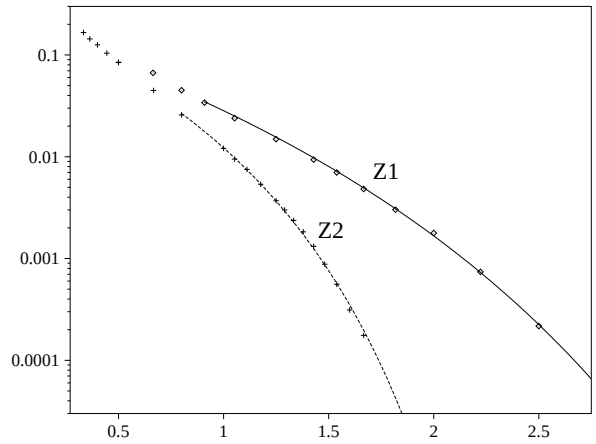

FIG. 6: An Arrhenius plot showing the temperature dependence of the diffusion constant for bulk Z1 and Z2 liquids, as labelled. The data points are simulation results and the solid lines are fits to the data using the VTF (Vogel-Tammann-Fulcher) equation, $D = D_0 \exp[BT_0/(T - T_0)]$.

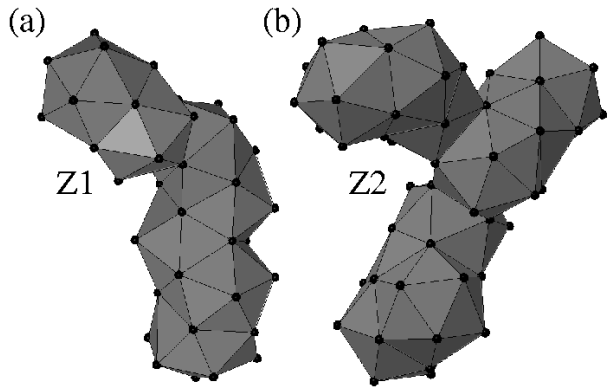

FIG. 7: Clusters of connected icosahedra that were located in the bulk liquids at T=1.0 and number density ρ=0.84. (a) a 53-atom cluster from the Z1 liquid and (b) a 73-atom cluster from the Z2 liquid.

below the temperature T_A a pronounced super-Arrhenius slowing down is observed. The non-Arrhenius part of the $D(T)$ curves extends for over two decades, thus demonstrating the pronounced glass-forming ability of the two systems simulated here. We also note that the activation energy, as estimated from the Arrhenius plot, is significantly larger in the case of the Z2 potential; this behaviour appears to be consistent with the larger amplitude of its Friedel-like oscillations.

Another issue that we addressed in these simulations was the formation of extended domains of icosahedral structure upon supercooling. The development of such domains has previously been demonstrated in simulations of a supercooled bulk liquid using the Dzugutov potential.[21,22] Moreover, these domains were found to be morphologically similar to the low-energy structures of isolated clusters for that potential.[23]

Here, we analyse atomic configurations obtained by steepest descent minimization of instantaneous atomic configurations representing equilibrium liquids. In order to discern icosahedral order in the first shell of neighbours, we first identified pentagonal bipyramids—pairs of neighbours with five common neighbours forming a closed ring (any two particles separated by the distance less than 1.5 were regarded as neighbours). A 13-atom icosahedron was identified as a central atom with 12 neighbours all of which form five-fold pairs (pentagonal bipyramids) with the central atom. Furthermore, we considered two icosahedra sharing at least 3 atoms as connected.

We found that both systems also demonstrate a clear tendency for the formation of extended icosahedral clusters upon cooling. This tendency is illustrated in Fig. 7 where we present typical clusters of connected icosahedra that develop upon supercooling of the two model liquids. For both systems, it is possible to observe a close similarity between the patterns of icosahedral aggregation in these clusters and those in the respective clusters presented in Figs. 3 and 4. We remark that the Z2 system clearly demonstrates, for both the isolated clusters and the icosahedral domains identified in the liquid, a more pronounced tendency for one-dimensional aggregation of icosahedra than the Z1 system.

IV. CONCLUSIONS

Following Frank,[40] we have sought insight into the structure of supercooled liquids by analysing the structures of the corresponding clusters; the clusters can allow the identification of the ideal, local structural order. This philosophy has also been employed in cluster models of the glass transition,[41] and has influenced theories such as the frustration-limited domain model.[42,43]

We have introduced two new potentials that are similar to effective potentials in metals with oscillations that lead to polytetrahedral and icosahedral order being preferred, thus making them good glass-formers. The cluster global minima generally correspond to non-compact arrangements of linked 13-atom icosahedra. For one potential (Z1) we find that two-dimensional networks of these icosahedra become preferred for the largest sizes we consider, whereas for the other potential (Z2) chains of icosahedra are only observed. Similar icosahedral aggregates were observed to form upon supercooling of the corresponding bulk liquids.

Along with the Dzugutov potential[14,15] and a modified version of it,[37] this series of potentials provides an ideal set of model systems to explore the relationship between the potential, the locally preferred structure, the energy landscape and the properties of supercooled liquids, such as fragility, glass-forming ability and the decoupling of diffusion and structural relaxation. Understanding these relationships has been a long-standing goal in the field of supercooled liquids, and simulations, here and in more

detail elsewhere,[26] confirm some of the expected correlations with the cluster structures we observe.

Acknowledgments

JPKD is grateful to the Royal Society for financial support. FHMZ and MD gratefully acknowledge support from the Swedish Research Foundation (VR).

* Electronic address: jpkd1@cam.ac.uk

1. C. A. Angell, J. Phys.-Condens. Mat. **12**, 6463 (2000).
2. P. G. Debenedetti and F. H. Stillinger, Nature **410**, 259 (2001).
3. S. Sastry, P. G. Debenedetti, and F. H. Stillinger, Nature **393**, 554 (1998).
4. F. Sciortino, W. Kob, and P. Tartaglia, Phys. Rev. Lett. **83**, 3214 (1999).
5. S. Sastry, Nature **409**, 164 (2001).
6. C. Donati, J. F. Douglas, W. Kob, S. J. Plimpton, P. P. H., and G. S. C., Phys. Rev. Lett. **80**, 2338 (1998).
7. C. Bennemann, C. Donati, J. Baschnagel, and S. C. Glotzer, Nature **399**, 246 (1999).
8. L. Santen and W. Krauth, Nature **405**, 550 (2000).
9. W. Kob and H. C. Andersen, Phys. Rev. Lett. **73**, 1376 (1994); Phys. Rev. E **51**, 4626 (1995), **52**, 4134 (1995).
10. T. F. Middleton, J. Hernández-Rojas, P. N. Mortenson, and D. J. Wales, Phys. Rev. B **64**, 184201 (2001).
11. T. F. Middleton and D. J. Wales, Phys. Rev. B **64**, 024205 (2001).
12. R. Di Leonardo, L. Angelani, G. Parisi, and G. Ruocco, Phys. Rev. Lett. **84**, 6054 (2000).
13. L. Angelani, R. Di Leonardo, G. Ruocco, A. Scala, and F. Sciortino, J. Chem. Phys. **116**, 10297 (2002).
14. M. Dzugutov, Phys. Rev. A **46**, R2984 (1992).
15. M. Dzugutov, J. Non-Cryst. Solids **156-158**, 173 (1993).
16. B. Sadigh, M. Dzugutov, and S. R. Elliott, Phys. Rev. B **59**, 1 (1999).
17. M. Dzugutov, Phys. Rev. Lett. **70**, 2924 (1993).
18. H. Jonsson and H. C. Andersen, Phys. Rev. Lett. **60**, 2295 (1988).
19. D. R. Nelson and F. Spaepen, Solid State Phys. **42**, 1 (1989).
20. F. Yonezawa, Solid State Phys. **45**, 179 (1991).
21. F. H. M. Zetterling, M. Dzugutov, and S. I. Simdyankin, J. Non-Cryst. Solids **293-295**, 39 (2001).
22. M. Dzugutov, S. I. Simdyankin, and F. H. M. Zetterling, Phys. Rev. Lett. in press (cond-mat/0109057).
23. J. P. K. Doye, D. J. Wales, and S. I. Simdyankin, Faraday Discuss. **118**, 159 (2001).
24. F. H. M. Zetterling, M. Dzugutov, and S. Lidin, MRS Symposium Proc. **643**, K9.5.1 (2001).
25. J. K. Brandon, R. Y. Brizard, P. C. Chieh, R. K. McMillan, and W. B. Pearson, Acta Cryst. B **30**, 1412 (1970).
26. S. I. Simdyankin and M. Dzugutov, unpublished.
27. J. Hafner, *From Hamiltonians to phase diagrams* (Springer-Verlag, Berlin, 1998).
28. J. A. Moriarty and M. Widom, Phys. Rev. B **56**, 7905 (1997).
29. J. P. K. Doye and D. J. Wales, J. Chem. Soc., Faraday Trans. **93**, 4233 (1997).
30. D. J. Wales and J. P. K. Doye, J. Phys. Chem. A **101**, 5111 (1997).
31. Z. Li and H. A. Scheraga, Proc. Natl. Acad. Sci. USA **84**, 6611 (1987).
32. D. J. Wales, J. P. K. Doye, A. Dullweber, M. P. Hodges, F. Y. Naumkin, F. Calvo, J. Hernández-Rojas and T. F. Middleton, The Cambridge Cluster Database, URL http://www-wales.ch.cam.ac.uk/CCD.html.
33. D. P. Shoemaker and C. B. Shoemaker, in *Introduction to Quasicrystals*, edited by M. V. Jaric (Academic Press, London, 1988), pp. 1–57.
34. F. C. Frank and J. S. Kasper, Acta Cryst. **11**, 184 (1958).
35. F. C. Frank and J. S. Kasper, Acta Cryst. **12**, 483 (1959).
36. J.-F. Sadoc and R. Mosseri, *Geometric Frustration* (Cambridge University Press, Cambridge, 1999).
37. J. P. K. Doye and D. J. Wales, Phys. Rev. Lett. **86**, 5719 (2001).
38. C. A. Angell, Science **267**, 1924 (1995).
39. This result can be proved by calculating the number of nearest neighbours in a chain of icosahedra as a function of N when linked in the different ways. $n^i_{\rm nn} = 26N/6 - 43/3$, $n^f_{\rm nn} = 42N/10 - 63/5$, $n^t_{\rm nn} = 50N/13 - 8$ where i, f and t stand for interpenetrating, face-sharing and tetrahedra bridged, respectively. For $N > 13$ $n^i_{\rm nn} > n^f_{\rm nn} > n^t_{\rm nn}$.
40. F. C. Frank, Proc. Royal Soc. London A **215**, 43 (1952).
41. G. J. Fan and H. J. Fecht, J. Chem. Phys. **116**, 5002 (2002).
42. D. Kivelson, S. A. Kivelson, X.-L. Zhao, Z. Nussinov, and G. Tarjus, Physica A **219**, 27 (1995).
43. D. Kivelson and G. Tarjus, Phil. Mag. B **77**, 245 (1998).